

## Cuboidal W<sub>3</sub>S<sub>4</sub> Cluster Complexes as New Generation X-ray Contrast Agents

Shi-Bao Yu, Michael Droege, Brent Segal, Sook-Hui Kim, Tony Sanderson, and Alan D. Watson\*

Torsten Almén Research Center, Nycomed Amersham Imaging, 466 Devon Park Dr., Wayne, Pennsylvania 19087

Received August 12, 1999

### Introduction

The existing generation of approved water soluble X-ray contrast agents, which includes such agents as iohexol, a nonionic monomer and iodixanol, a nonionic dimer, are all based on the triiodobenzene platform.<sup>1–3</sup> These types of materials have been available for the last 45 years and have tremendously improved the clinical utility of X-ray imaging. However, there has been no groundbreaking progress in the research and development of new classes of soluble X-ray contrast agents for almost 20 years. We have been exploring for some time the use of heavy metal ( $Z > 53$ ) cluster complexes to provide a new generation of X-ray contrast agents, based on their superior X-ray attenuation characteristics when compared to iodine-based agents.<sup>4</sup> The cuboidal, trinuclear tungsten cluster [W<sub>3</sub>Q<sub>4</sub>]<sup>4+</sup> (Q = O, S) has been explored as an entry point to a new generation of X-ray contrast agents based on its synthetic accessibility, stability, and presumed ability to strongly bind polyaminopolycarboxylate ligand systems.<sup>5–11</sup>

### Experimental Section

**Materials and Synthesis.** All chemicals were used as received. The nona-aqua ion [W<sub>3</sub>S<sub>4</sub>(H<sub>2</sub>O)<sub>9</sub>]Cl<sub>4</sub> (**1**) was prepared through a modification of literature procedures to facilitate scale-up,<sup>5,11</sup> and has been reported elsewhere.<sup>12</sup> The solid **1** can be stored in a freezer for very long periods (>2 years) with no noticeable degradation.

Na<sub>2</sub>[W<sub>3</sub>S<sub>4</sub>(TTHA)] (**2**), H<sub>2</sub>[W<sub>3</sub>S<sub>4</sub>(TTHA)] (**3**), and (NMG)<sub>2</sub>[W<sub>3</sub>S<sub>4</sub>(TTHA)] (**4**). To the green solution of 10 g (10.1 mmol) **1** in 600 mL of DMF was added 5 g (10.1 mmol) of TTHA.<sup>13</sup> The mixture was heated to reflux for 3 h, and a purple solid separated from the solution. This solid was collected and dissolved in water, NaOH (1 N) was added

Table 1. Crystallographic Data for [(W<sub>3</sub>S<sub>4</sub>)<sub>2</sub>(TTHA)<sub>2</sub>]<sup>4+</sup> (**5**)

formula	C <sub>36</sub> H <sub>69</sub> N <sub>8</sub> O <sub>40</sub> Na <sub>3</sub> S <sub>8</sub> W <sub>6</sub>
fw	2682.6
temperature	−95 °C
λ (Å)	0.71073
space group	P2 <sub>1</sub> /c
a (Å)	13.348(6)
b (Å)	16.737(8)
c (Å)	15.810(7)
β (deg)	98.42(3)
V (Å <sup>3</sup> )	3494(5)
Z	2
D <sub>calcd</sub> (g/cm <sup>3</sup> )	2.55
R; R <sub>w</sub> (F <sup>2</sup> > 2.5σ(F <sup>2</sup> ))	6.44%; 5.88%
GO F	1.56

to adjust the pH to 7, and insoluble materials were filtered off. The filtrate was passed through an ion exchange column (AG50 × 8, Na<sup>+</sup> form, 400 mL resin) to complete the exchange of Me<sub>2</sub>NH<sub>3</sub><sup>+</sup> to Na<sup>+</sup>. The solvent was removed by rotary evaporation, and the residue was dissolved in a minimal amount of water. It was loaded onto a Sephadex column (G-15, 600 mL resin) and was eluted with water. The second distinct purple band (a minor fraction) was collected and was purified by repeated passages through a size exclusion column. The pure solid **2** was isolated by rotary evaporation with a 17% (2.1 g) yield. UV–vis λ<sub>max</sub>, nm (ε, M<sup>−1</sup>cm<sup>−1</sup>): 313 (6200), 445 (340), 573 (560). <sup>183</sup>W NMR (D<sub>2</sub>O, 70 °C, δ, ppm in reference to Na<sub>2</sub>WO<sub>4</sub>): 2394.9, 2422.2, 2897.0. Cation exchange of **2** to **3** was generally quantitative. Anal. of **3**. Calcd for C<sub>18</sub>H<sub>26</sub>N<sub>4</sub>O<sub>12</sub>W<sub>3</sub>S<sub>4</sub>: C, 18.48; H, 2.24; N, 4.79; W, 47.13; S, 10.96. Found: C, 18.40; H, 2.38; N, 4.69; W, 47.06; S, 10.88. MS (FAB, M+H<sup>+</sup>): Calcd, 1171; found, 1171. The neutralization of **3** to produce **4** was always carried out *in situ* and a yield of 100% was assumed.

**HPLC Conditions.** Ion pairing reverse phase, C18 columns; mobile phase: 36% aqueous MeOH containing 10 mM tetrabutylammonium bromide (TBAB), monitored at 240 nm.

**X-ray Crystallographic analysis of Na<sub>3</sub>H[(W<sub>3</sub>S<sub>4</sub>)<sub>2</sub>(TTHA)<sub>2</sub>·16H<sub>2</sub>O (**5**).** A summary of selected crystallographic data for **5** is given in Table 1. Deep purple, platelike crystals of **5** were obtained by slow crystallization from aqueous solution of **2**. One of them, 0.05 × 0.18 × 0.20 mm, was mounted on a glass fiber using Paratone N hydrocarbon oil. An Enraf-Nonius CAD-4 Diffractometer, equipped with a N<sub>2</sub> flow low-temperature device was used to collect 5055 raw intensity data. They were converted to structure factors by correction for scan speed, background, and Lorentz and polarization effects. The Patterson method was used to solve the structure, and its refinement was done using standard least-squares and Fourier techniques. The final residuals were obtained using 2547 accepted data points for 220 variables.

### Results and Discussion

**Synthesis.** A mixture of **1** and TTHA in DMF was heated to reflux for 3 h to produce a purple solid that is a complicated mixture of metal cluster complexes (W<sub>3</sub>S<sub>4</sub>)<sub>x</sub>(TTHA)<sub>y</sub>. Subsequent workup using ion exchange and size exclusion chromatography techniques isolated the pure solid, **2**, in yields of around 15%. The protonated salt **3** was prepared by cation exchange, and subsequent neutralization with two molar equivalents of NMG afforded **4**. The use of DMF as solvent is critical in the preparation of **2** since the slow decomposition of DMF at reflux temperature produces sufficient dimethylamine to act as both a means of deprotonating TTHA as well as supplying a counterion to the crude product. The first size exclusion chromatography step separated **2** (contained in a second, minor fraction) from those complexes with higher molecular weights (the first, major, fraction). Repeated chromatographic workup of the minor

- (1) Grainger, R. G. *Br. J. Radiol.* **1982**, *55*, 1.
- (2) Balszkiewicz, P. *Invest. Radiol.* **1994**, *29* (S1), S51.
- (3) Almén, T. *Invest. Radiol.* **1994**, *29* (S1), S37.
- (4) Almén, T.; Berg, A.; Christofferson, J.-O.; Droege, M.; Kim, S.-H.; Krautwurst, K.-D.; Segal, B.; Watson, A.; Yu, S.-B. Manuscript in preparation.
- (5) Segawa M.; Sasaki, Y. *J. Am. Chem. Soc.* **1985**, *107*, 5565.
- (6) Shibahara, T.; Kohda, K.; Ohtsujii, A.; Yasuda, K.; Kuroya, H. *J. Am. Chem. Soc.* **1986**, *108*, 2757.
- (7) Dori, Z.; Cotton, F. A.; Llusar, R.; Schwotzer, W. *Polyhedron* **1986**, *5* (3), 907.
- (8) Shibahara, T.; Takeuchi, A.; Kuroya, H. *Inorg. Chim. Acta* **1987**, *127*, L39.
- (9) Shibahara, T.; Takeuchi, A.; Kunitomo, T.; Kuroya, H. *Chem. Lett.* **1987**, 867.
- (10) Nasreldin, M.; Olatunji, A.; Dimmock, P. W.; Sykes, A. G. *J. Chem. Soc., Dalton Trans.* **1990**, 1765.
- (11) Shibahara, T.; Yamasaki, M.; Sakane, G.; Minami, K.; Yabuki, T.; Ichimura, A. *Inorg. Chem.* **1992**, *31*, 640.
- (12) Yu, S.-B.; Droege, M.; Segal, B.; Downey, S.; Sanderson, T.; Fellmann, J.; Watson, A. *Inorg. Chim. Acta* **1997**, *263*, 61.
- (13) Abbreviations: TTHA, triethylene tetraamine hexaacetate; EDTA, ethylenediamine tetraacetate; EGTA, ethylene glycol diamine tetraacetate; NMG, *N*-methyl-D-glucamine; CT, computer tomography; MRI, magnetic resonance imaging.

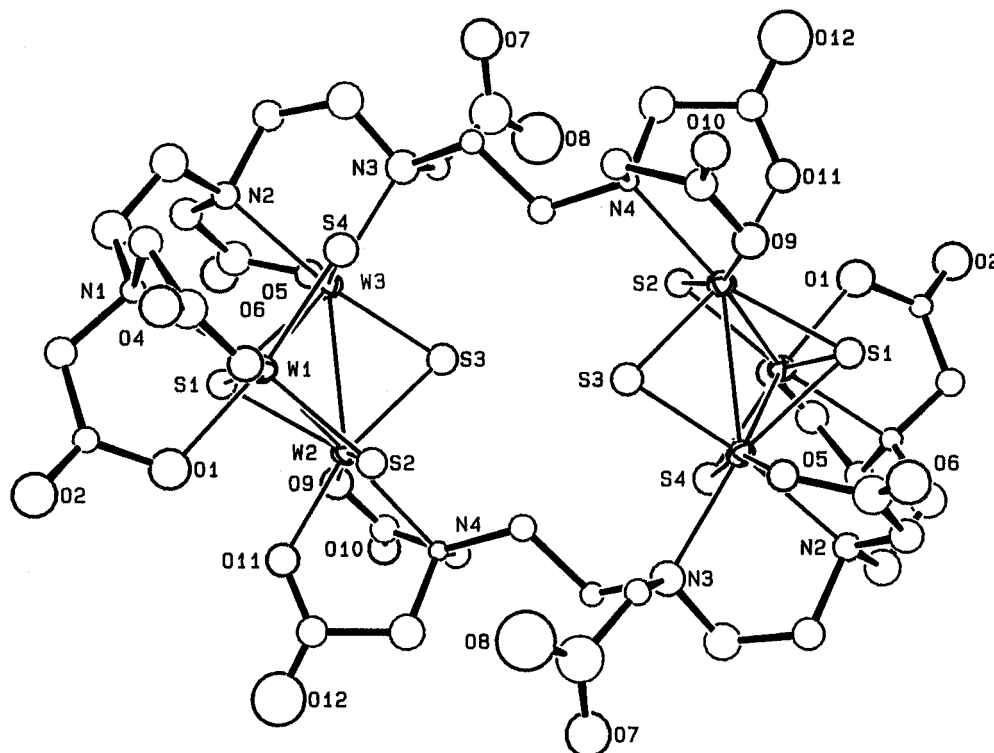
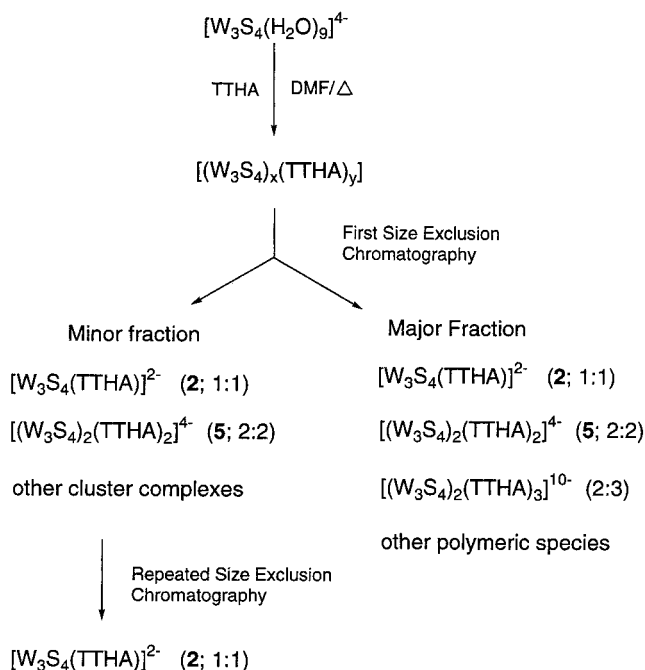


**Figure 1.** Structure of  $[(W_3S_4)_2(TTHA)_2]^{4-}$  anion, showing 50% thermal ellipsoids and partial atom labeling scheme.

**Scheme 1.** Preparation and Isolation of  $[W_3S_4(TTHA)]^{2-}$



fraction produced the pure 1:1 ( $W_3S_4$ /ligand) cluster complex **2** (Scheme 1). Since this complexation reaction involves a trinuclear cluster with nine coordination sites and a decadentate ligand, it is not surprising that the yield of **2** is low, with the majority of the reaction products as polymeric higher molecular weight complexes.

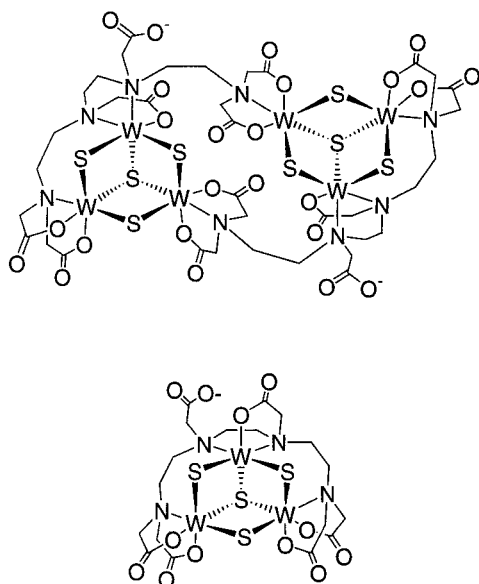
Samples of the  $[W_3S_4(TTHA)]^{2-}$  complex obtained after different stages of purification were analyzed by HPLC and by mass spectrometry (FAB and ESI) techniques. After an initial pass through a size exclusion column, FAB and ESI showed the  $Na^+$  and  $H^+$  molecular ions corresponding to  $[(W_3S_4)_2(TTHA)_2]^{4-}$  were contained in the minor fraction, in addition

to the  $[W_3S_4(TTHA)]^{2-}$  species, while HPLC identified three or more additional minor impurities. HPLC identified the complex **2**, together with lower molecular weight impurities as minor components in the major fraction, with a large proportion of the major fraction consisting of complexes of higher molecular weights. In addition, ESI identified molecular ions corresponding to  $[(W_3S_4)_2(TTHA)_3]^{10-}$  in the major fraction. Finally, a sample of purified  $Na_2[W_3S_4(TTHA)]$  was analyzed by analytical ultracentrifugation using sedimentation equilibrium techniques and an 1:1 ( $W_3S_4$ /ligand) stoichiometry of the cluster complex was established by its molecular weight in solution  $\{MW = 1249 \pm 31$  vs calcd 1214).

**Description of Structures.** Attempts to grow single crystals of the monomeric  $[W_3S_4(TTHA)]^{2-}$  complex have, to date, been unsuccessful. However, crystals of the dimeric cluster **5** were obtained from the slow evaporation of an aqueous solution of **2**. The crystals were subjected to an X-ray crystallographic analysis and the resulting structure (Figure 1) provides the first known example of two  $M_3Q_4$  ( $M = Mo, W$ ) clusters both complexed and linked by two polyaminopolycarboxylate ligands to form a 2:2 cluster–ligand complex. The only other examples of dimeric  $M_3Q_4$  ( $Q = O, S$ ) polyaminopolycarboxylate complexes are  $[(Mo_3O_4)_2(EDTA)_3]^{4-}$  and  $[(W_3S_4)_2(EGTA)_3]^{4-}$ , in which three EDTA or EGTA ligands link two  $M_3Q_4$  units to provide 2:3 cluster–ligand complexes.<sup>12,14</sup> The  $[(W_3S_4)_2(TTHA)_2]^{4-}$  anion contains a crystallographically imposed inversion center in the center of the molecule which relates the two complexed  $W_3S_4$  units. The decadentate TTHA ligand coordinates one  $W_3S_4$  unit in a hexadentate fashion and the other  $W_3S_4$  unit in a tridentate fashion to link two  $W_3S_4$  units. Within each  $W_3S_4$  unit, two tungsten atoms are coordinated by two IDA (iminodiacetate) units of TTHA. Due to spatial constraints, one of the IDA units coordinates the tungsten atom in an unusual fashion; the central nitrogen atom is not in the usual *trans* position to the  $\mu_3$ -S atom, rather it is in the *cis* position {S1–

**Table 2.** Selected Bond Lengths (Å) and Angles (deg) for  $[(W_3S_4)_2(TTHA)_2]^{4-}$ 

Bond Lengths			
W1–W2(W3)	2.718 (2)	W2–W3	2.774(2)
W1–S1	2.367(7)	W1–S2	2.287(7)
W2–S1	2.350(7)	W1–S4	2.250(9)
W3–S1	2.387(8)	W3–S3	2.298(8)
W2–S2	2.309(7)	W3–S4	2.289(8)
W2–S3	2.309(8)	W1–O1	2.15(2)
W1–N1	2.34(2)	W1–O3	2.13(2)
W2–O9	2.13(2)	W3–O5	2.09(2)
W2–O11	2.06(2)	W3–N2	2.29(2)
W2–N4	2.28(2)	W3–N3	2.37(3)
Angles			
W–W–W	59.30(4)–61.39(5)	S1–W–S(2,3,4)	103.8 (3)–107.6(3)
S(2,3,4)–W–S(2,3,4)	96.8(3)–102.6(3)	S1–W1–O1	88.0(6)
S1–W1–O3	157.1(5)	S1–W1–N1	87.2(5)
S1–W2–N4	158.4(6)	S1–W2–O9(O11)	87.2(5) (89.3(6))
S1–W3–O5	85.2(6)	S1–W3–N2	84.4(6)
S1–W3–N3	161.8(6)	S(2,3,4)–W–(O,N) <sub>cis</sub>	82.9(6)–91.6(6)
S(2,3,4)–W–(O,N) <sub>trans</sub>	159.3(6)–160.7(5)	O,N–W–O,N	71.6(7)–82.1(8)

**Figure 2.** Schematic drawings of  $[(W_3S_4)_2(TTHA)_2]^{4-}$  (upper) and  $[W_3S_4(TTHA)]^{2-}$  (lower).

W1–N1, 87.2(5)°) and *trans* to a  $\mu_2$ -S atom {S2–W1–N1, 160.4(5)°}. The middle section of the TTHA binds to one tungsten atom with the two amine nitrogen atoms and one carboxylate oxygen. All available coordination sites on the two  $W_3S_4$  units are completely occupied by donor atoms from these two TTHA ligands, with two pendant carboxylate groups remaining uncoordinated. Selected bond distances and angles are listed in Table 2.

The crystal structure of **5** provided a template from which a rational structure of **2** could be deduced. The schematic drawings for both structures are depicted in Figure 2. The proposed structure of **2** is also supported by the results of a  $^{183}W$  NMR (Figure 3) study. Three  $^{183}W$  peaks were observed, indicating that the three tungsten atoms are in different environments. Two  $^{183}W$  signals at the 2400 ppm range correspond to the two tungsten atoms with N,O,O ligation, and the one at 2900 ppm arises from the tungsten atom with N,N,O ligation. This is a rare example of a case where a metal cluster can be viewed as a single metal ion with all available coordination sites on the  $W_3S_4$  unit being completely complexed by donor atoms from one linear TTHA ligand. The closest known prior examples of this type of multidentate ligand coordination to a metal cluster are the iron–sulfur clusters in metalloproteins<sup>15</sup> (where the

protein is viewed as a single ligand) and the established synthetic chemistry of iron–sulfur clusters with macrocyclic ligands<sup>16</sup> or peptides.<sup>17</sup>

**Biological Studies.** In contrast to the aqua ion **1**, which decomposes quickly even in 1 N HCl solution and anaerobic conditions, complex **2** is remarkably stable in aqueous solutions in air between pH 2 and pH 10. It exhibited no degradation (monitored by UV–vis) in aqueous solution (pH 7) for more than 60 days even when incubated at 37 °C in air. The solubility of the cluster complexes **2** and **4** in water (pH 7) were determined to be 0.169 and 0.488 M, respectively.

The central synthetic rationale behind the development of a number of clinically useful MRI contrast agents<sup>18</sup> and radiopharmaceuticals<sup>19</sup> has been the chelation of a single metal ion generally by one or two appropriate organic ligands to provide a safe pharmaceutical agent which would be well tolerated by the human body, with a pharmacokinetic profile that is largely derived from the physical properties of the chelating ligands to provide the desired biodistribution. Chelation of the heavy metal  $W_3S_4$  cluster with the TTHA ligand produced a novel complex with the desired physicochemical profile. The *iv* LD<sub>50</sub> (the dose that is lethal to 50% of the tested animals when administered intravenously) in mice for the cluster complexes **2** and **4** were respectively determined to be 6.5 mmol/kg and 7.2 mmol/kg, which provides a greater than 5-fold safety margin for a drug candidate at a hypothetical imaging dose of around 1 mmol/kg.

*In vitro* and *in vivo* (rat) comparative studies performed on commercial CT scanners indicated that the X-ray attenuation capability of the tungsten core in the cluster complex **2** is twice that of iohexol on a molar basis, validating predictions based on theoretical calculations.<sup>20</sup> The *in vivo* comparative study in

(15) Beinert, H.; Holm, R. H.; Munck, E. *Science* **1997**, *277*, 6.

(16) (a) Holm, R. H. *Pure Appl. Chem.* **1998**, *70*, 931. (b) Tomohiro, T.; Uoto, K.; Okuno, H. *J. Chem. Soc., Dalton Trans.* **1990**, 2459.

(17) (a) Que, L., Jr.; Anglin, J. R.; Bobrik, M. A.; Davison, A.; Holm, R. H. *J. Am. Chem. Soc.* **1974**, *96*, 6042. (b) Mulholland, S. E.; Gibney, B. R.; Rabanal, F.; Dutton, P. L. *J. Am. Chem. Soc.* **1998**, *120*, 10296. (c) Ueyama, N.; Fuji, M.; Sugawara, T.; Nakamura, A. *Pept. Chem.* **1986**, *23*, 269.

(18) See, e.g.: (a) Rocklage, S. M.; Watson, A. D.; Carvlin, M. J. In *Magnetic Resonance Imaging*; Stark, D. D., Bradley, W. G., Eds.; Morsby Year Book, 1992; p 372. (b) Lauffer R. B. *Chem. Rev.* **1987**, *87*, 901.

(19) See, e.g.: (a) Schubiger, P. A.; Alberto, R.; Smith, A. *Bioconjugate Chem.* **1996**, *7*, 165. (b) Schwochau, K. *Angew. Chem., Int. Ed. Engl.* **1994**, *33*, 2258. (c) Jurisson, S.; Berning, D.; Jia, W.; Ma, D. *Chem. Rev.* **1993**, *93*, 1137.

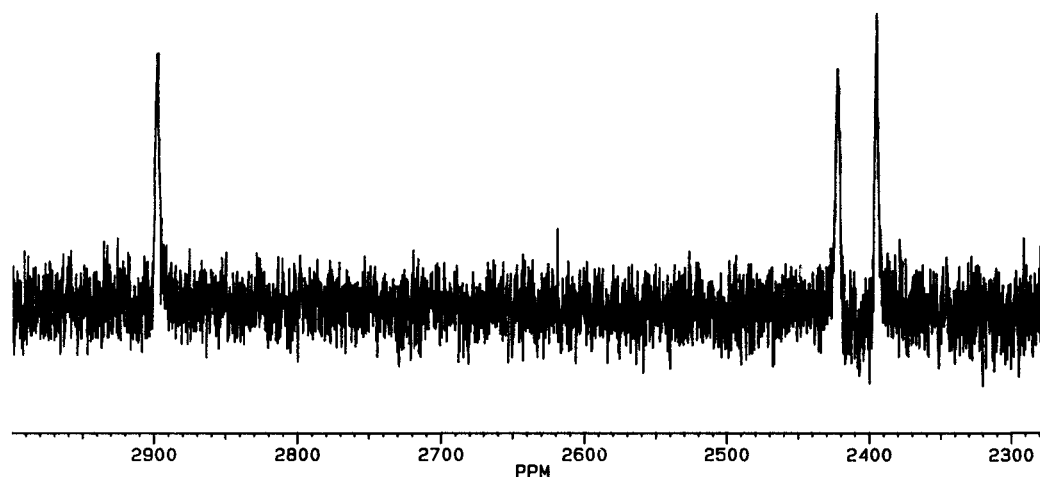


**Figure 3.**  $^{183}\text{W}$  NMR spectrum of  $[\text{W}_3\text{S}_4(\text{TTHA})]^{2-}$ .

rats also demonstrated that the cluster complex **2** has a two-compartment extracellular pharmacokinetic profile similar to that of the commercial agent iohexol.<sup>21</sup>

**Concluding Remarks.** In summary, the aqua ion **1** can be reproducibly prepared in large quantities and stored conveniently. A highly pure  $\text{W}_3\text{S}_4$ -TTHA complex with 1:1 stoichiometry can be obtained through a novel, simple reaction pathway followed by complex anion isolation using size exclusion chromatography. Chelation of the  $\text{W}_3\text{S}_4$  unit by the

TTHA ligand imparts the necessary degree of water solubility and chemical stability under physiological conditions. Furthermore, the heavy metal cluster complexes **2** and **4** have demonstrated suitably low acute toxicities in mice and, for complex **2**, an acceptable pharmacokinetic profile. The superior X-ray contrast efficacy of heavy metal cluster complexes such as **2** was confirmed by *in vitro* and *in vivo* X-ray imaging studies. Currently, this synthetic approach is being extended to other  $\text{M}_3\text{Q}_4$ -polyaminopolycarboxylate complexes, and their possible utility as the next generation X-ray contrast agents is under further exploration.

**Acknowledgment.** We thank Dr. F. Hollander of University of California, Berkeley (X-ray crystal structure determination) and Dr. E. H. Braswell of University of Conn. (Solution molecular weight determination) for experimental assistance.

**Supporting Information Available:** HPLC traces from the purification steps of **2** and listings of crystallographic data, positional and thermal parameters, and bond lengths and angles for **5**. This material is available free of charge via the Internet at <http://pubs.acs.org>.

IC990976G

(20) The prediction was based on the integration of mass X-ray attenuation coefficients for tungsten and iodine over the useful X-ray photon energy range ( $\sim 50$ – $120$  keV) used in clinical diagnostic imaging. Tungsten's X-ray attenuation coefficient is much greater above its K-edge (69 keV) than iodine, which makes it overall a better X-ray attenuator. This property, high attenuation power at higher X-ray photon energies, of heavy metal clusters has another important clinical application. Its use could potentially reduce the radiation dose to patients since the probability of high-energy X-ray photons to penetrate, rather than being absorbed by a human body is greater than that of low-energy photons.

(21) Almén, T.; Golman, K. In *Contrast Media: Biological Effects and Clinical Application*; Parvez, Z., Moncada, R., Sovak, M., Eds.; CRC Press: Boca Raton, 1987; Vol. 1, Chapter 6, p 77.